Chapter 2
The Rich Chemistry of the Copper and Zinc Sites in PrP^C

Glenn L. Millhauser

Abstract Research over the last two decades demonstrates clearly that the function of the cellular form of the prion protein, PrP^C, is related to its ability to bind copper and zinc. Zinc (Zn^{2+}) coordination is homogeneous and localized to the octarepeat domain, with participation of the histidine side chains. In contrast, copper uptake is complex and dependent on the oxidation state of the metal ion (Cu^+ or Cu^{2+}) and its concentration. This chapter will cover a brief history of PrP^C–metal interactions leading to the current structural models, Cu^{2+}-promoted structural features that protect against PrP^C neurotoxicity, a recently recognized relationship between Cu^{2+} coordination and inherited prion disease arising from octarepeat inserts, assessment of PrP-copper electrochemical features, with insight into the basis of PrP^C neuroprotection and transmembrane signaling, and recent findings of how copper participates in the regulation of PrP^C proteolysis.

Keywords Prion · Zinc · Copper · Nuclear magnetic resonance · Electron paramagnetic resonance · Proteolysis · Protein structure · Neurotoxicity · Electrochemistry · Electrophysiology

2.1 Introduction

Research over the last two decades continues to find remarkable functional roles for the normal cellular form of the prion protein (PrP^C). PrP^C supports myelin development (Bremer et al. 2010), influences sleep-wake cycles (Tobler et al. 1996), is upregulated at sites of ischemic injury (McLennan et al. 2004), promotes neuron

G. L. Millhauser (✉)
Department of Chemistry & Biochemistry, University of California Santa Cruz, Santa Cruz, CA, USA
e-mail: glennm@ucsc.edu

W.-Q. Zou, P. Gambetti (eds.), *Prions and Diseases*,
https://doi.org/10.1007/978-3-031-20565-1_2

development (Kanaani et al. 2005), protects nerve cells against chemical and oxidative assaults (Klamt et al. 2001; Rachidi et al. 2003), and modulates select transmembrane proteins (Watt et al. 2012; Kuffer et al. 2016; Evans and Millhauser 2017; Salzano et al. 2019). Although one cannot yet assign a sole function to PrP^C as, say, a signaling molecule, enzyme, or transporter, it is clear that the protein is required for normal neurological function. Most functional investigations link PrP^C to metal ion binding, specifically to copper and zinc. This link was emphasized in an elegant X-ray fluorescence study that examined the spatial location and relative levels of iron, copper, and zinc in mouse brain (Pushie et al. 2011). Comparison of wild-type, PrP knockouts (KO), and 20× overexpressers revealed remarkable differences in specific brain regions, with each metal ion exhibiting a unique PrP-dependent profile. For example, PrP appears to drive copper levels near the ventricles and thalamus, whereas zinc is upregulated in cortical regions. And while there is scant evidence suggesting that PrP^C directly binds iron, its levels are nevertheless influenced by PrP expression, perhaps suggesting a relationship between distinct metal transporters, as established in yeast (Bleackley and Macgillivray 2011).

This chapter will begin with a brief historical review of the PrP metal ion literature, with emphasis on works that frame current thinking. Next, I will describe the biophysical features of the copper and zinc sites in PrP^C. Unlike most other metal binding proteins that present a single, well-defined high-affinity site, PrP responds dynamically with a rich variation of coordination modes that depend on metal concentration and the presence of competing species. Recognition of these distinct coordination modes provides new insight into inherited disease resulting from octarepeat inserts. I will also describe electrochemical work that not only provides a detailed characterization of PrP-copper redox properties but also suggests a mechanism for PrP-mediated signaling. This chapter will conclude with new findings that reveal the role of metal ions in PrP^C proteolysis.

2.2 Brief History

PrP^C is able to bind both copper and zinc, but most studies emphasize the specific interaction with Cu^{2+}. (Note: Copper possesses two common, biologically relevant oxidation states: Cu^+ and Cu^{2+}.) Hornshaw et al. recognized that the histidine-rich octarepeat domain, containing four tandem PHGGGWGQ segments, would likely bind Cu^{2+}, and demonstrated this directly with mass spectrometry (Hornshaw et al. 1995a, b). Moreover, they showed a persistent 1:1 complex, although it was also noted that the OR region could take up additional equivalents. Next, using circular dichroism (CD), which detects conformational changes, and fluorescence quenching, they estimated a Cu^{2+} dissociation constant in the low micromolar range (Hornshaw et al. 1995a, b).

In 1997, Brown et al. published a landmark study that clearly identified a physiological connection between PrP and copper (Brown et al. 1997). First, using a peptide corresponding to the PrP N-terminal domain, PrP(23-98), they showed that

the protein takes up multiple Cu^{2+} equivalents with positive cooperativity, described by an unusually high Hill coefficient. Estimated affinity was higher than initially found by CD, as reflected in a low, submicromolar dissociation constant. Brown and colleagues further compared brain copper levels between wild-type and KO mice and reported a severe reduction in brain copper in the transgenics. Many aspects of this work have been revisited in the last 20+ years, but there is little doubt that this initial publication firmly established PrP^C as a copper metalloprotein.

The lowered copper content in the mouse KO suggested that perhaps PrP^C functions as a transporter. PrP^C is attached to membrane surfaces through a GPI anchor and is cycled from the extracellular space to early endosomes through endocytosis, with approximately 90% of the protein returned to the surface by exocytosis. As monitored in N2a mouse neuroblastoma cells, Pauly and Harris showed that addition of 200 μM copper stimulated rapid PrP^C internalization, while removal of the metal ion allowed the protein to redistribute back to the membrane surface (Pauly and Harris 1998). Elimination of the octarepeats, or the His residues within the repeats, fully disrupts these copper-dependent processes (Perera and Hooper 2001). Similarly, certain mutations in the octarepeat domain that give rise to familial prion disease also interfere with copper-stimulated endocytosis (Perera and Hooper 2001). Collectively, these findings suggest that PrP^C may play a key role in copper trafficking. However, early examinations of tissue copper, and copper protein activity, in brain fractions derived from wild-type and transgenic mice possessing different levels of PrP^C failed to find a correlation between PrP^C expression and copper levels (Waggoner et al. 2000). Consequently, this promising line of research did not progress. However, the X-ray fluorescence imaging work described in the "Introduction" section, certainly motivated a renewed look at the role of PrP^C in neuronal copper distribution.

In parallel to cellular assays were several notable structural and biophysical investigations (Stöckel et al. 1998; Viles et al. 1999; Aronoff-Spencer et al. 2000; Van Doorslaer et al. 2001; Burns et al. 2002, 2003; Garnett and Viles 2003; Valensin et al. 2004; Chattopadhyay et al. 2005). Early work focused primarily on the octarepeat domain, although newer research finds copper sites outside of this region. Viles et al. performed a wide array of spectroscopic experiments including CD, nuclear magnetic resonance (NMR), and electron paramagnetic resonance (EPR) (Viles et al. 1999). This work demonstrated a 1:1 stoichiometry between each histidine (His) containing repeat segment and Cu^{2+} and suggested a micromolar dissociation constant. Moreover, they identified a strong pH dependence, with tight copper binding only at pH 6.0 and above. These findings have endured many follow-up studies. To account for cooperative uptake, they proposed a ring-like structure of alternating His imidazole side chains and Cu^{2+} ions. While there is precedence for this type of structure in the inorganic chemistry literature, it is now considered unlikely to be a significant biological conformation.

Most copper-binding proteins exhibit a very high affinity, reflected by a low dissociation constant (K_d). For example, the K_d for copper at the active site of superoxide dismutase is approximately 10^{-14} M. Early work with PrP N-terminal peptides pointed to a much weaker affinity, suggesting that perhaps PrP might not take up

copper in vivo. This was addressed with detailed MS and fluorescence assays to carefully assess copper binding thermodynamics in full-length PrP (Kramer et al. 2001). Analysis of the observed fluorescence quenching revealed both affinity and detailed stoichiometry, with five Cu^{2+} per protein. Copper uptake showed positive cooperativity with the last equivalent exhibiting a K_d of ~2 μM, well below the level of Cu^{2+} in blood estimated at 18 μM. It is not clear, though, how relevant the comparison to blood copper levels is, given that high levels of PrP are localized to extracellular pre-synaptic surfaces in the CNS (Herms et al. 1999). As will be discussed, more recent analyses find specific binding modes that display very high affinity, below 1.0 nM, and thus further establishing that PrP takes up Cu^{2+} in vivo.

Several recent investigations point to the role of PrP^C as a metal-ion-dependent modulator of signal transduction. For example, Watt et al. demonstrated that Zn^{2+} binding to PrP^C enhances zinc transmembrane transport through the AMPA receptor, a member of the multi-subunit glutamate receptor family (Watt et al. 2012, 2013). PrP^C has also been found to modulate transmembrane currents through NMDA receptors in a copper-dependent fashion. Specifically, copper-occupied PrP^C reduces the NMDA receptor's sensitivity to glycine, a ligand that otherwise promotes persistent cationic currents (Stys et al. 2012; You et al. 2012). Legname and coworkers find that PrP^C exhibits neuronal growth factor activity controlling direction and rate of neurite projections (Kanaani et al. 2005; Nguyen et al. 2019). This function is abolished by mutagenesis of the histidine residues required for copper and zinc coordination.

2.3 Features of Cu^{2+} and Zn^{2+} Coordination in PrP

Copper binds within PrP's N-terminal region, with the relevant segment from the human sequence shown below:

PrP (51-111) PQGGGGWGQ(P**H**GGGWGQ)4GGGT**H**SQWNKPSKPKTNMK**H**

There are five tandem eight-residue repeats, each with the canonical sequence PXGGGWGQ, but in the first repeat, a Gln fills the X position. Since the imidazole side chain of histidine is required for copper uptake, the first repeat does not participate in copper coordination. Thus, from a sequence or genetics perspective, there are five N-terminal octarepeats, but from a metal ion coordination perspective, there are four. Beyond the octarepeat domain, copper also interacts with high affinity at the His residues at positions 96 and 111 (Jones et al. 2005, Walter et al. 2009). The current consensus is that all copper coordination is within the segment PrP(61-111) (human) bounded by the histidines (His, bold H) in the sequence shown above.

A number of early investigations used peptide design, NMR, mass spectrometry, circular dichroism, Raman spectroscopy, molecular modeling, and related biophysical approaches to develop insight into the structure of the Cu^{2+}-octarepeat complex. Ultimately, though, EPR provided the essential insights leading to the current models. EPR is sensitive to the chemical environment at paramagnetic Cu^{2+} centers and,

through hyperfine couplings to copper's unpaired electron, can directly reveal nearby nuclei and atomic features of the coordination environment. Details of the relevant EPR techniques have been reviewed elsewhere (Millhauser 2004, 2007); a summary of the coordination features is given in Fig. 2.1. The copper coordination environment depends critically on the ratio of copper to protein. At low copper concentrations, the four octarepeat His imidazole side chains bind simultaneously to a single Cu^{2+}, as shown in the figure and inset (Chattopadhyay et al. 2005). This is often referred to as the low occupancy binding mode or "component 3," based on component analysis of the EPR spectra. The affinity for this mode is very high, with a dissociation constant of approximately 0.10 nM (Walter et al. 2006).

At intermediate Cu^{2+} concentration, the octarepeats take up two copper equivalents, with each coordinated by two His side chains (not shown) (Chattopadhyay et al. 2005). At high copper concentrations, the octarepeat domain saturates at four equivalents, with each His binding to a single Cu^{2+}, as shown in Fig. 2.1 (Aronoff-Spencer et al. 2000; Burns et al. 2002, 2003; Chattopadhyay et al. 2005). This high

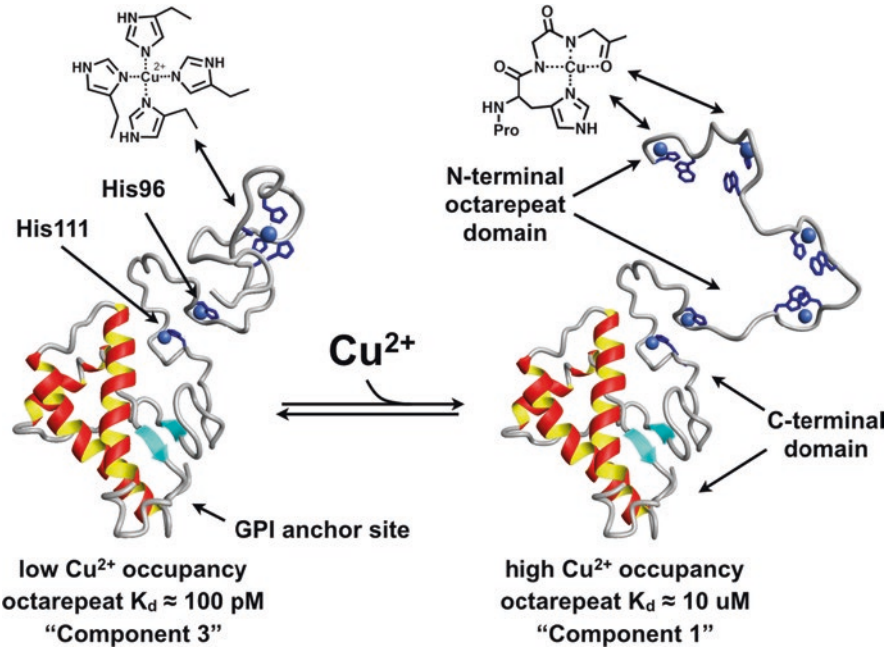

Fig. 2.1 Structural features of PrP^C at low and high Cu^{2+} concentrations. The C-terminal domain is helical, whereas the N-terminal domain is flexible and able to restructure to accommodate different copper coordination modes. At low [Cu^{2+}], the metal ion coordinates to sites localized to His96 and His111. In addition, a single equivalent of Cu^{2+} binds within the octarepeat domain, coordinated by the four His imidazole side chains ("component 3," details shown in the inset). The affinity in the octarepeat domain is high, as characterized by a low K_d of approximately 100 pM. At high [Cu^{2+}], the octarepeat domain restructures to take up four copper equivalents, each coordinated to single His side chain and backbone nitrogens ("component 1," inset). The affinity for this coordination mode is lower than that of component 3

occupancy binding mode is referred to as "component 1." The copper affinity for this state is lower than that of component 3, with a dissociation constant of approximately 10 μM (Walter et al. 2006). The specific coordination features of this high occupancy site, shown in the inset, were determined by isotopic labeling, in combination with a range of EPR techniques (Aronoff-Spencer et al. 2000), and confirmed by X-ray crystallography of the Cu^{2+}-HGGGW complex (Burns et al. 2002).

The specific features of the component 1 site are unusual compared to previously characterized protein copper sites. In most copper metalloproteins, the metal ion is coordinated to His or Cys side chains. For example, copper superoxide dismutase contains the metal ion with four tetrahedrally placed His imidazoles. As seen in the Fig. 2.1 inset, the Cu^{2+} ion coordinates to the His side chain, the deprotonated amide nitrogens of the two Gly residues that immediately follow the His, and a Gly carbonyl. In addition, there is an axially coordinated water molecule that hydrogen bonds to the Trp indole hydrogen (not shown). A coordination sphere with deprotonated amides has been seen previously with the N-terminal copper binding segment of albumin (Harford and Sarkar 1997), and also in peptides, but not in the interior polypeptide segments of a protein. The involvement of amide nitrogens confers significant pH sensitivity since an increase in the H^+ concentration (lower pH) protonates at the nitrogen and competes with copper complexation. Consequently, high occupancy copper binding is unstable below pH ~ 6.0. It has been proposed that this might provide a chemical mechanism for release of Cu^{2+} in the endosomal compartments (Burns et al. 2002).

In addition to Cu^{2+} uptake in the octarepeats, there are two additional binding sites localized to His96 and His111 (human PrP numbering), and these also exhibit sub-nanomolar affinity. These two sites are often referred to as the "5th sites," since early studies suggested that only the involvement of His96, beyond that of the four sites in the octarepeat domain (Burns et al. 2003). We prefer to label these as "non-octarepeat" coordination sites, thus underscoring their distinct location and chemical properties (Walter et al. 2009). At both of these non-octarepeat sites, copper coordinates to the imidazole side chain, the His backbone nitrogen, and two additional backbone nitrogens from the residues on the N-terminal side of the His (Burns et al. 2003). Affinity at these sites is high with a K_d that is similar to that found for the multi-His component 3 mode in the octarepeat domain. Titration studies show that these non-octarepeat sites take up copper simultaneously with component 3 (Walter et al. 2009). Once PrP^C is saturated with Cu^{2+}, the octarepeat domain restructures to component 1 coordination, thus enabling additional binding equivalents, as shown in Fig. 2.1.

Like copper, zinc also binds to PrP^C and stimulates endocytosis (Pauly and Harris 1998). Because this metal ion is found only as diamagnetic Zn^{2+}, EPR is of limited use in directly evaluating its coordination features. To address this, we applied several complementary approaches. First, using an octarepeat peptide, as well as full-length PrP^C, we competed Zn^{2+} against Cu^{2+} and monitored by copper EPR. Interestingly, we found that regardless of concentration, Zn^{2+} was not able to displace Cu^{2+}, which shows that copper has a much higher affinity than zinc (Walter et al. 2007). However, Zn^{2+} was able to influence the Cu^{2+} coordination mode,

shifting the distribution to favor component 1 binding. Next, we tested Zn^{2+} coordination to a range of octarepeat-derived peptides and monitored binding with the reagent diethylpyrocarbonate (DEPC) (Walter et al. 2007), which chemically modifies free imidazole groups, but only if they are not involved in metal ion coordination. Analysis by mass spectrometry showed protection against DEPC modification only with the full octarepeat domain. Collectively, these experiments demonstrate that Zn^{2+} coordinates to the four octarepeat His imidazoles, equivalent to that observed for Cu^{2+} in its low occupancy mode. With a K_d of approximately 200 μM, the affinity is substantially lower than any of the coordination modes found for Cu^{2+}. However, because Zn^{2+} competes with Cu^{2+}, it is able to influence copper coordination in a concentration-dependent fashion. These results, summarized in the scheme in Fig. 2.2, show that when copper levels are low, PrP can simultaneously bind both copper and zinc. At higher copper levels, the protein accommodates the zinc by shifting to the high occupancy binding mode that minimizes the ratio of histidines to copper. However, when no rearrangement can accommodate both zinc and the available copper, it is the zinc that is displaced, not the copper. Finally, Markham et al. used ^{113}Cd (nuclear spin = ½) as a Zn surrogate for NMR studies (Markham et al. 2019). Cd, like Zn, is in group 12 of the periodic table and therefore forms a stable divalent cation. Analysis of the ^{113}Cd chemical shifts and $^2J_{NH}$ scalar couplings confirmed the expected octarepeat His coordination through the ε2 nitrogen.

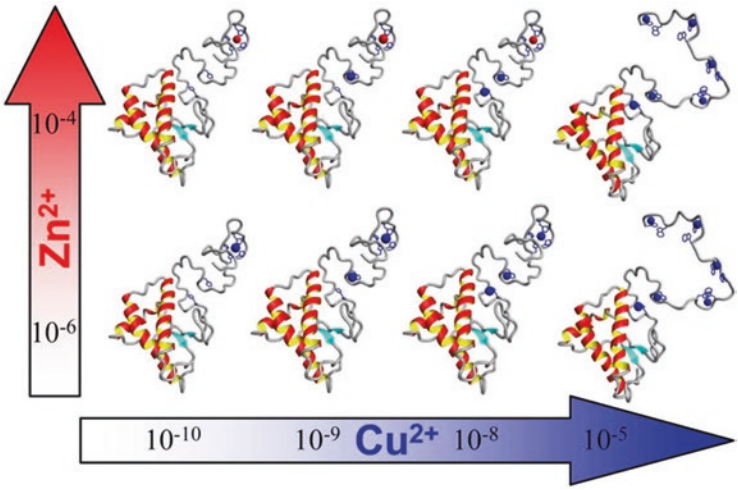

Fig. 2.2 Models representing metal binding in the N-terminal domain of PrP. Top row (High Zinc); Zinc (red) is bound by the octarepeat region (left) while non-octarepeat sites (H96 and H111) are available for copper binding (blue, middle). Copper at high concentrations will displace zinc from octarepeats to form up to four equivalents of component 1 (right). Bottom row (low zinc); copper (blue) is bound by the octarepeats in component 3 when copper is low (left), with increasing copper loads the non-octarepeat sites (middle). High copper (right column) results in component 1 copper binding by the octarepeats. Approximate molar metal concentrations are shown in the arrows

Companion isothermal titration calorimetry (ITC) experiments performed with Zn^{2+} gave a measured K_d between 17 μM and 40 μM, suggesting a somewhat higher affinity than that previously measured by DEPC competition experiments. Interestingly, NMR chemical shifts, binding assays, mutagenesis, and companion molecular dynamics studies implicated the C-terminal residue E199 (E200 in the human sequence) as participating in the Cd second coordination sphere through a salt-bridge with a His imidazole δ1 NH.

It was originally thought that the PrP^C N-terminal and C-terminal domains were structurally independent of each other. Consequently, it was expected that both copper and zinc would interact solely with the octarepeat domain and, in the case of copper, the non-octarepeat segments surrounding His96 and His111, as well. However, the independence of these two protein domains was brought into question by Sonati et al. who showed that C-terminally directed monoclonal antibodies (mAbs) modulated N-terminus-driven toxicity, as demonstrated in both cerebellar organotypic murine brain slices and in mice (Sonati et al. 2013). This led to a functional model of PrP^C, which describes the protein as possessing an N-terminal toxic effector domain and a C-terminal regulatory domain. These results pointed to a physical interaction between the PrP^C N- and C-terminal domains that are responsible for arresting inherent N-terminus-promoted toxicity. Coincident with these findings, Spevacek et al. reported magnetic resonance investigations into potential, Zn^{2+}-mediated higher-order structure in PrP^C (Spevacek et al. 2013). ^1H-^{15}N-HSQC experiments in the presence of Zn^{2+}, which binds solely to the octarepeat domain, found that the presence of the metal ion led to significant line broadening of cross-peak signals from C-terminal residues. Moreover, the affected residues were localized to a well-defined patch on C-terminal helices 2 and 3. Double Electron-Electron Resonance (DEER) EPR of PrP^C with nitroxide labels engineered into the N- and C-terminal domains confirmed that Zn^{2+} addition brings these two protein segments into close proximity. Together, these experiments suggest that the surfaces of C-terminal helices 2 and 3 form a critical patch to which the Zn^{2+} occupied octarepeat binds, in turn suppressing N-terminal PrP^C toxicity. Interestingly, the implicated patch is negatively charged, thus providing an electrostatic driving force for interaction with the Zn^{2+}-occupied octarepeat, and also carries the majority of missense mutations (>60%) that confer inherited prion disease (Spevacek et al. 2013).

It was subsequently shown that copper binding to PrP^C also drives a strong interaction between the protein's N- and C-terminal domains, as shown in Fig. 2.3 (Evans et al. 2016; Wu et al. 2017; McDonald et al. 2019; Schilling et al. 2020). EPR, NMR, and mass spectrometric characterization of this Cu^{2+}-promoted *cis* interaction further supports involvement of the C-terminal patch identified by the prior studies with zinc. Moreover, the epitope of the POM1 mAb, identified as highly toxic by Sonati et al. (2013), overlaps the C-terminal surface that would otherwise contact the copper-occupied octarepeat domain (Evans et al. 2016).

A number of PrP mutants with polypeptide deletions in the central region, between the copper/zinc-binding octarepeat domain and the globular C-terminal domain, are found to be remarkably toxic, producing a neonatal lethal phenotype in transgenic mice (Shmerling et al. 1998). In addition, whole-cell patch clamp

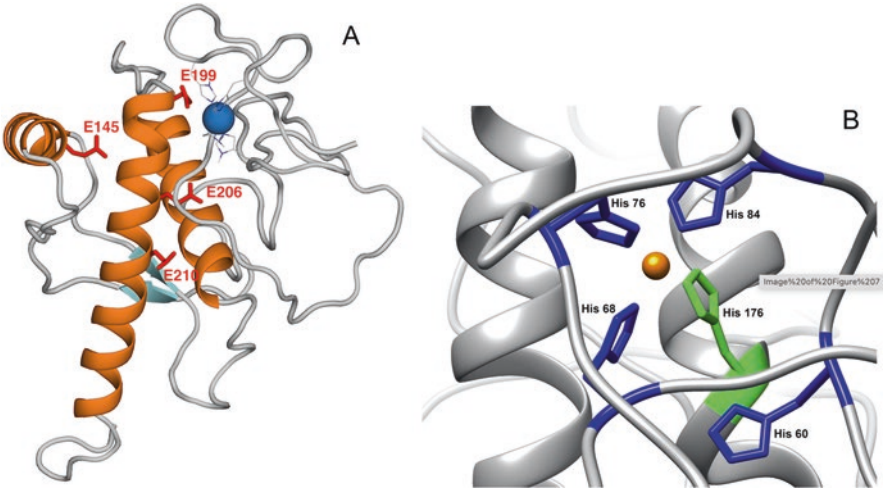

Fig. 2.3 Copper stabilizes a neuroprotective interaction between the N-terminal and C-terminal PrP^C domains. (**a**) Representative structure from an MD trajectory of MoPrP(54–230), with Cu^{2+} bound as multi-His (component 3) in the N-terminal OR. The interdomain structure is stabilized by interaction between the OR-bound Cu^{2+} ion and acidic residues on helix 3 (E199, E206, and E210). (**b**) Detailed EPR analysis finds that Cu^{2+} coordination arises from three octarepeat His residues (blue) and one C-terminal His at position 176 (green)

electrophysiological measurements find that transfection of these mutants in various cell lines and cultured neurons produces large, spontaneous, transmembrane cationic currents, mediated by the polybasic PrP N-terminus (residues 23-31) (Solomon et al. 2010). Rescue of these currents is achieved by co-transfection with wild-type PrP. Of the various deletion mutants studied thus far, Δ105-125 (ΔCR), is particularly toxic, requiring the largest amount of wild-type PrP for rescue. A central hypothesis arising from these studies is that the metal ion-promoted *cis* interaction holds the N-terminal residues away from the plasma membrane, thus restricting the formation of transmembrane pores. This was tested directly with both biophysical and electrophysiological approaches. NMR showed that ΔCR-PrP^C exhibited a substantially reduced Cu^{2+}-promoted *cis* interaction, as indicated by a loss of line-broadened residues in ^{1}H-^{15}N-HSQC spectra (Wu et al. 2017). Cross-linking mass spectrometry showed that Cu^{2+} organizes the N-terminal domain in a conformation that would sequester residues 23-31 away from the plasma membrane (McDonald et al. 2019). In parallel, spontaneous currents from ΔCR-PrP transfected into the N2a neuroblastoma cells were suppressed by the addition of Cu^{2+} in the form of copper-pentaglycine (Wu et al. 2017); however, deletion of the octarepeat domain eliminated current suppression by copper. Given that ΔCR-PrP produces a phenotype consistent with aspects of genuine prion disease, these findings provide compelling evidence that the copper/zinc-promoted *cis* interaction stabilizes PrP^C in its proper, non-neurodegenerative conformational state.

Molecular details of the Cu^{2+}-promoted *cis* interaction are only now beginning to emerge. With component 3 copper coordination (Cu^{2+}:PrP = 1:1), the copper center retains its formal 2+ charge and consequent electrostatic interaction with the negatively charged patch on the regulatory C-terminal domain. Schilling et al. noticed that this patch also possesses two conserved His residues, H139 and H176 (mouse sequence), that might offer further stabilization by direct coordination with the copper center (Schilling et al. 2020). NMR experiments performed on PrP with these residues mutated to Tyr reveal a clear weakening of *cis* interaction, yet, a suite of pulsed EPR experiments find conservation of the four-His coordination shell. Together, these observations demonstrate that the component 3 copper site in full-length PrP^C is comprised of three octarepeat histidines and one C-terminal histidine, as shown in Fig. 2.3. Moreover, whole-cell patch clamp experiments find that elimination of these two His residues in PrP-expressing neuroblastoma (N2a) cells leads to enhanced spontaneous currents. We therefore conclude that copper acts as a bridge linking the PrP effector and regulatory domains and that this interaction is further stabilized by complementary electrostatic forces.

2.4 A Role for Altered Copper Coordination in Octarepeat Expansion Disease

Approximately 10–15% of human TSE cases are inherited and arise from mutations in the open reading frame of the *PRNP* gene (Prusiner 2004). Of these, most are missense mutations in the folded C-terminal domain. For example, the E200K mutation causes midlife development of CJD with most patients dying 6–24 months after onset (Colombo 2000). In addition to these, point mutations are insertional mutations of one to nine PHGGGWGQ segments in the octarepeat domain (Goldfarb et al. 1991). This class of mutations is enigmatic insofar that they modify a region of the protein that is not essential for propagating prion disease. Treatment of PrP^{Sc} with proteinase K cleaves the protein at approximately residue 90, thereby removing the octarepeat domain, but the remaining protease-resistant aggregate retains infectivity. Despite these results, early studies with transgenic mice showed that the PrP octarepeats modulate the disease process. Specifically, inoculated mice expressing a modified PrP^C lacking residues 32–93 develop disease but with longer incubation times than wild-type, produce tissues with lower prion titers and a reduced presentation of prion plaques (Flechsig et al. 2000).

Disease progression in individuals with octarepeat expansions depends on the number of inserts. Individuals with one to four extra octarepeats develop disease with an average onset age of 64 years, whereas five to nine extra octarepeats result in an average onset age of 38 years, a difference of almost three decades (Croes et al. 2004; Kong et al. 2004). A number of previous studies examined the biophysical properties of expanded octarepeat domains with emphasis on either the rate of amyloid production or its uncomplexed backbone conformation (Leliveld et al.

2006, 2008; Dong et al. 2007). However, none of these identified a quantitative link between octarepeat length and age of disease onset.

Given the profound influence of octarepeat domain length on expansion disease, we explored whether the domain's response to copper is altered by insertion number (Stevens et al. 2009). We also reevaluated all known cases of human prion disease resulting from octapeptide insertions and compared the findings to biophysical studies that examined the balance between component 1 and component 3 coordination, as a function of octarepeat domain length. Beginning with statistical data from two existing studies (Croes et al. 2004; Kong et al. 2004), we surveyed the clinical literature, pooled the data, and established a new data set covering approximately 30 families and 108 individuals. Onset age for individual cases are shown in Fig. 2.4a. The red line is drawn at 55.5 years. All cases of up to four octarepeat inserts (eight repeats total) are above this line, and 96% of the cases of five or more octarepeat inserts are below the line. Although there is significant scatter in reported onset age for each specific octarepeat length, the dramatic shift to early onset disease between four and five inserts is apparent. A detailed statistical analysis shows that the results are indeed consistent with the presence of two groups, one composed of individuals with 1 to 4 OR inserts and another of individuals with 5 to 8 inserts (Stevens et al. 2009).

We then performed EPR analysis on a series of PrP-derived constructs from four to nine repeats, corresponding to zero to five insertions. The experiments showed that domains with 4–7 repeats (i.e., zero to three insertions) behave much like the wild-type. However, constructs of 8 or 9 repeats exhibit persistent component 3 coordination. Moreover, these constructs take up approximately twice as much copper as the wild type. Equivalent trends were observed with full-length recombinant

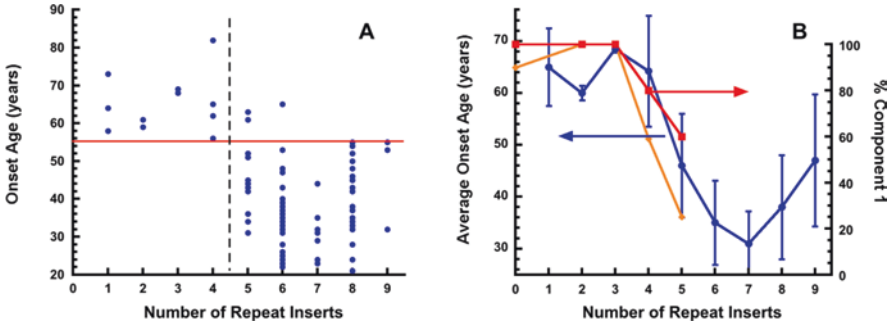

Fig. 2.4 The relationship between onset age for familial prion disease resulting from octarepeat inserts and copper coordination modes. (**a**) Onset age for individual cases as a function of extra octarepeat inserts. Note that wild-type corresponds to four repeats, so three inserts correspond to seven total repeat segments. The horizontal red line is at 55.5 years and represents a statistically defined separation between late and early onset. (**b**) Average onset age, with standard deviation (blue circles, left axis), and component 1 coordination (orange diamonds and red squares, right axis, for 3.0 and 4.0 equivalents Cu^{2+}, respectively) as a function of extra octarepeat inserts. At both copper concentrations, component 1 coordination drops suddenly at approximately the same OR length threshold as average onset age

protein, where we compared wild-type with mutant PrP^C containing 5 repeat inserts. To underscore these findings, we compared the average onset age and standard deviation, as a function of octarepeat length, to Cu^{2+} binding properties. The longest OR expansions favor component 3 coordination and resist component 1. Thus, component 1 coordination serves as a convenient measure of altered Cu^{2+} binding properties. Figure 2.4b shows the relative population of component 1 coordination for each OR construct superimposed on the average age of onset. For wild-type and expansions involving up to seven repeats (three inserts beyond wild-type), component 1 coordination is dominant for both 3.0 and 4.0 equivalents Cu^{2+}. However, at eight and nine ORs (four and five inserts, respectively), the population of component 1 coordination drops precipitously.

These data reveal a remarkable relationship, where decreased onset age and persistent component 3 coordination take place at threshold of eight or more total repeats. It is possible, therefore, that our findings suggest an important protective role for component 1 coordination that may be lost in cases of octarepeat expansion disease with four or more inserts. However, the recent work by Schilling et al provides a different perspective (Schilling et al. 2020). In their analysis of how C-terminal His residues stabilize the protective N-term—C-term *cis* interaction through a bridging copper ion, they recognized that expansion of the N-terminal octarepeats could diminish this otherwise protective interdomain contact. NMR analysis of PrP^C with octarepeat insertions found that up to three additional octarepeat segments did not weaken the observed *cis* interaction. However, at four or five insertions, which marks the transition to early onset prion disease, NMR evidence of the interaction was essentially eliminated. Consequently, with four or more insertions, both component 1 binding *and* the protective interdomain *cis* interaction are reduced. Together, these findings motivate a careful examination of the distinct chemical properties and reactivity of component 1 vs component 3 copper coordination, and further strengthen the hypothesis that the copper-mediated *cis* interaction is critical for arresting inherent PrP^C neurotoxicity.

2.5 Electrochemical Properties of the PrP Copper Sites

Copper's ability to cycle between the Cu^+ and Cu^{2+} oxidation sites is essential for life. For example, cellular respiration relies on cytochrome c oxidase, a copper-dependent enzyme that converts molecular oxygen to water ultimately leading to the production of ATP. Since the earliest studies connecting PrP^C to copper uptake, there has been interest in understanding reduction-oxidation (redox) cycling at the copper sites. One line of inquiry suggests that PrP^C functions as a superoxide dismutase (SOD), which inactivates toxic O_2^- converting it to the more benign hydrogen peroxide (H_2O_2). This hypothesis has been controversial and is reviewed elsewhere (Daniels and Brown 2002; Brown 2009). The connection between copper coordination mode and onset age for octarepeat expansion disease, discussed above, certainly motivates an evaluation as to whether component 1 and component 3 coordination sites give rise to distinct redox properties.

Initial electrochemical studies used cyclic voltammetry to evaluate short single repeat peptides as models of component 1 coordination (Bonomo et al. 2000). Reduction of Cu^{2+} to Cu^{+} was found to be energetically unfavorable, leading to the possibility that PrP^C may stabilize copper in its oxidized form. From a neuroprotective perspective, this could be important since weakly complexed copper readily cycles between oxidation states resulting in the production of reactive oxygen species (ROS) that are often cytotoxic. By stabilizing copper in a single oxidation state, PrP^C may quench this deleterious chemistry.

Component 3 coordination, with four His residues, appears somewhat similar to the active site in SOD and initially suggested that it might readily undergo redox cycling. Redox kinetics, as measured by bathocuproine absorbance, suggested that indeed component 3 was more easily reduced than component 1 (Miura et al. 2005). Building from these results, it was proposed that PrP^C might function in concert with endocytosis as a copper reductase. In this scenario, extracellular Cu^{2+} binds to PrP^C with component 1 coordination, and the complex is internalized by endocytosis. Next, the low pH drives rearrangement in the octarepeat domain to favor component 3 coordination, leading to reduction to Cu^{+}. Finally, the copper is released and internalized through a copper transporter.

In collaborative work with Zhou and coworkers, we revisited the detailed electrochemical features of component 1 and component 3 coordination modes (Liu et al. 2011). The full octarepeat domain with one equivalent of Cu^{2+} served as a model for component 3 coordination. Cyclic voltammetry performed in the presence of ascorbate, with and without oxygen, and under nearly reversible conditions showed facile reduction to Cu^{+}, along with a significant increase in affinity. Thus, as opposed to cycling copper, these data suggest that Cu^{+} is very stable in this low occupancy mode, and unlikely to be reoxidized back to Cu^{2+}. Next, we used the same conditions to examine component 1 coordination and found reduction potentials consistent with a copper center that supports cycling between its oxidation states. However, when we compared the findings to free copper or simple copper-peptide complexes like those found in blood or cerebral spinal fluid, we observed that the reaction was controlled and less likely to produce cytotoxic species such as hydroxyl radicals. Additional assays demonstrated that copper bound to PrP with component 1 coordination, under reducing conditions by ascorbate, gently converts dissolved oxygen to hydrogen peroxide. A summary of these findings is shown in Fig. 2.5.

The ability to bind copper and facilitate redox cycling is shared with the Aβ peptide and α-synuclein, which are causative in Alzheimer's and Parkinson's diseases, respectively. Unlike PrP^C, however, these species exhibit only a single binding mode and, therefore, a single profile for producing hydrogen peroxide. Comparing coordination modes identified for these two neurodegenerative species with those for PrP^C, we find that component 3 in PrP^C is by far the least reactive, producing hydrogen peroxide at the lowest rate, whereas component 1 is the most reactive (Liu et al. 2011). Thus, PrP^C exhibits vastly different electrochemical profiles, depending on copper occupancy. Both modes are neuroprotective, with component 3 coordination completely inhibiting copper redox activity and component 1 regulating activity with the controlled formation of hydrogen peroxide.

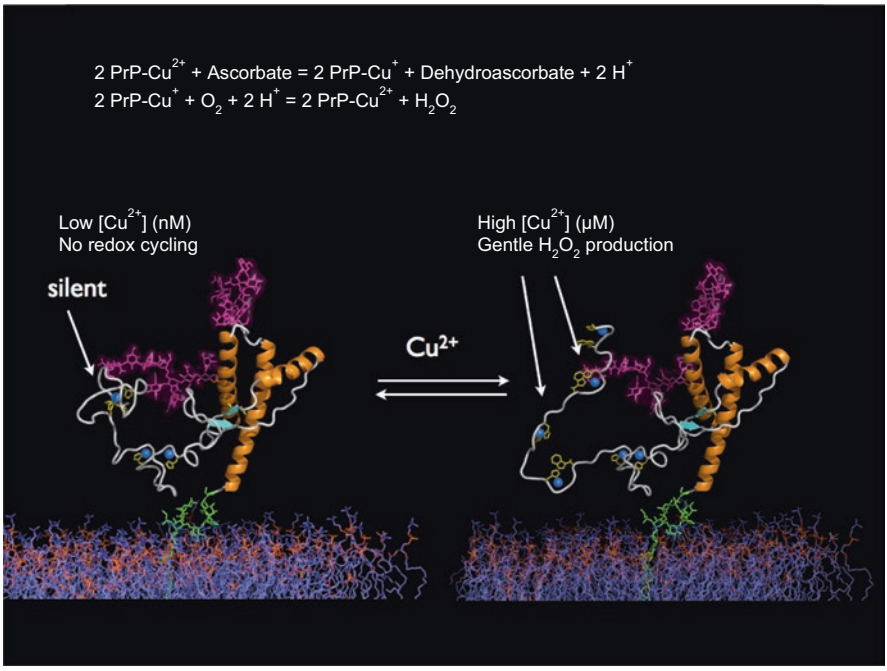

Fig. 2.5 Schematic representation of the possible roles of PrP^C–Cu^{2+} complexes in quenching the Cu^{2+} redox cycling or gradual production of H_2O_2 for signal transduction. PrP is tethered to cell membrane via the GPI anchor (green) with its α-helices in the C terminus shown in orange, N-linked carbohydrates in purple, and the N-terminal copper binding segment depicted in white. When [Cu^{2+}] is at a low level (nM or lower), Cu^{2+} (blue sphere) remains bound in the component 3 mode (left), quenching the Cu^{2+} redox cycling. At higher [Cu^{2+}] (μM) the binding mode transitions to component 1 (right), leading to a gradual and controlled production of H_2O_2

Together, these findings support a role for PrP^C in suppressing copper's inherent redox activity that would otherwise be very damaging to cellular components. However, the discovery that high copper occupancy PrP^C produces hydrogen peroxide suggests additional biochemical control. Similar to nitric oxide, hydrogen peroxide is now considered a signaling species of particular importance in the immune system and also in protein localization (Veal et al. 2007). There are likely several possible mechanisms for H_2O_2 action. For example, PrP^C has been linked to transmembrane signaling (Mouillet-Richard et al. 2000) and it is noteworthy that hydrogen peroxide readily crosses membrane bilayers and inactivates phosphatase and kinase active sites by reaction with catalytic residues.

2.6 Copper Regulation of PrP^C Proteolytic Cleavage

PrP^C undergoes enzymatic cleavage at two well-defined sites leading to detectable truncated forms in vivo. One proteolysis site resides between K109-H110 (mouse sequence), termed α-cleavage, and produces the N-terminal and C-terminal fragments, N1 and C1, respectively. The preponderance of recent evidence suggests that α-cleavage, which separates most of the flexible PrP N-terminus from the folded C-terminus, is due to action from one or more members of the ADAM (A Disintegrin And Metalloproteinase) family of enzymes, specifically ADAM8, ADAM10, and ADAM17. Among these, ADAM8 is established as responsible for α-cleavage in skeletal muscle tissue (Liang et al. 2012). The domains released by α-cleavage exhibit potent activities. The N1 fragment is antiapoptotic, possibly acting through the inhibition of caspase-3 (Guillot-Sestier et al. 2009). Conversely, the C1 fragment promotes apoptosis through p53-dependent caspase-3 activity, although it appears as though the protective effects of N1 significantly outweigh the pro-apoptotic effects of C1 (Sunyach et al. 2007). Perhaps more importantly, substoichiometric levels of C1 protect against PrP^{Sc} propagation.

PrP^C also undergoes β-cleavage, which takes place at multiple sites within and immediately following the octarepeat domain, producing N2 and C2 fragments (Chen et al. 1995). Experiments with different cell lines expressing PrP^C find that levels of C2 are greatly enhanced upon the addition of peroxide, suggesting proteolysis by reactive oxygen species (ROS) generated by intrinsic copper (McMahon et al. 2001; Watt and Hooper 2005). A separate pathway to β-cleavage of PrP^{Sc} is enzymatic, produced by calpains (Yadavalli et al. 2004) and cathepsin (Dron et al. 2010) proteases. In general, β-cleavage is observed in normal brain tissue, but C2 is enriched in prion infection. Unlike the N1 and C1 fragments, N2 and C2 do not show any bioactivity or neuroprotection, although β-cleavage's production of N2 and C2 may indirectly assert a biological effect by prohibiting the formation of N1.

The prevailing paradigm of PrP^C cleavage posits that α-cleavage is enzymatically driven and constitutes normal processing, while β-cleavage results from aberrant copper redox activity and is associated with the development of prion disease. But the identification of several ADAM family enzymes producing α-cleavage, along with the structural features promoted by copper and zinc, motivated a reassessment of PrP^C proteolysis. Interestingly, detailed analysis of the resulting proteolytic products found that α-cleavage does not take place at a single site but, instead, may take place at one of three proximal sites, termed α1, α2 and α3, depending on the specific ADAM enzyme and added metal ion (McDonald et al. 2013). Importantly, both Cu^{2+} and Zn^{2+} suppress β-cleavage, in turn favoring α-cleavage, thereby providing yet an additional mechanism by which these physiologic metal ions inhibit aberrant, neurotoxic signaling of the prion protein (McDonald et al. 2013).

The cumulative findings reviewed here emphasize the complex connection between zinc and copper uptake and the variability in copper binding as controlled by concentration. The relationship between copper coordination modes and the observed onset age for prion disease, which is associated with octarepeat expansion,

suggests that metal ion regulation may also factor into the development of disease. New electrochemical findings provide a foundation for understanding how PrP^C protects cells against oxidative assaults and also reveal a possible mechanism for transmembrane signaling, while detailed studies of PrP^C proteolysis find that metal ions may be crucial for inhibiting deleterious protein degradation pathways. Further refinement of these concepts is sure to lead to a precise function for PrP^C and perhaps new insights into how the loss of function contributes to neurodegenerative disease.

Acknowledgments This work was supported by NIH grant R35 GM131781. The author wishes to thank Professor F. Zhou of California State University, Los Angeles, and Ms. Amy Freiberg, UC Santa Cruz for helpful insights and editorial comments.

References

Aronoff-Spencer E, Burns CS, Avdievich NI, Gerfen GJ, Peisach J, Antholine WE, et al. Identification of the Cu^{2+} binding sites in the N-terminal domain of the prion protein by EPR and CD spectroscopy. Biochemistry. 2000;39:13760–71.

Bleackley MR, Macgillivray RT. Transition metal homeostasis: from yeast to human disease. Biometals. 2011;24(5):785–809.

Bonomo RP, Impellizzeri G, Pappalardo G, Rizzarelli E, Tabbi G. Copper(II) binding modes in the prion octarepeat PHGGGWGQ: a spectroscopic and voltammetric study. Chem Eur J. 2000;6:4195–202.

Bremer J, Baumann F, Tiberi C, Wessig C, Fischer H, Schwarz P, et al. Axonal prion protein is required for peripheral myelin maintenance. Nat Neurosci. 2010;13(3):310–8.

Brown DR. Brain proteins that mind metals: a neurodegenerative perspective. Dalton Trans. 2009;21:4069–76.

Brown DR, Qin K, Herms JW, Madlung A, Manson J, Strome R, et al. The cellular prion protein binds copper in vivo. Nature. 1997;390:684–7.

Burns CS, Aronoff-Spencer E, Dunham CM, Lario P, Avdievich NI, Antholine WE, et al. Molecular features of the copper binding sites in the octarepeat domain of the prion protein. Biochemistry. 2002;41:3991–4001.

Burns CS, Aronoff-Spencer E, Legname G, Prusiner SB, Antholine WE, Gerfen GJ, et al. Copper coordination in the full-length, recombinant prion protein. Biochemistry. 2003;42(22):6794–803.

Chattopadhyay M, Walter ED, Newell DJ, Jackson PJ, Aronoff-Spencer E, Peisach J, et al. The octarepeat domain of the prion protein binds Cu(II) with three distinct coordination modes at pH 7.4. J Am Chem Soc. 2005;127(36):12647–56.

Chen SG, Teplow DB, Parchi P, Teller JK, Gambetti P, Autilio-Gambetti L. Truncated forms of the human prion protein in normal brain and in prion diseases. J Biol Chem. 1995;270(32):19173–80.

Colombo R. Age and origin of the PRNP E200K mutation causing familial Creutzfeldt-Jacob disease in Libyan Jews. Am J Hum Genet. 2000;67(2):528–31.

Croes EA, Theuns J, Houwing-Duistermaat JJ, Dermaut B, Sleegers K, Roks G, et al. Octapeptide repeat insertions in the prion protein gene and early onset dementia. J Neurol Neurosurg Psychiatry. 2004;75(8):1166–70.

Daniels M, Brown DR. Purification and preparation of prion protein: synaptic superoxide dismutase. Method Enzymol. 2002;349:258–67.

Dong J, Bloom JD, Goncharov V, Chattopadhyay M, Millhauser GL, Lynn DG, et al. Probing the role of PrP repeats in conformational conversion and amyloid assembly of chimeric yeast prions. J Biol Chem. 2007.

Dron M, Moudjou M, Chapuis J, Salamat MK, Bernard J, Cronier S, et al. Endogenous proteolytic cleavage of disease-associated prion protein to produce C2 fragments is strongly cell- and tissue-dependent. J Biol Chem. 2010;285(14):10252–64.

Evans EGB, Millhauser GL. Copper- and zinc-promoted interdomain structure in the prion protein: a mechanism for autoinhibition of the neurotoxic N-terminus. Prog Mol Biol Transl Sci. 2017;150:35–56.

Evans EG, Pushie MJ, Markham KA, Lee HW, Millhauser GL. Interaction between prion protein's copper-bound octarepeat domain and a charged C-terminal pocket suggests a mechanism for N-terminal regulation. Structure. 2016;24(7):1057–67.

Flechsig E, Shmerling D, Hegyi I, Raeber AJ, Fischer M, Cozzio A, et al. Prion protein devoid of the octapeptide repeat region restores susceptibility to scrapie in PrP knockout mice. Neuron. 2000;27(2):399–408.

Garnett AP, Viles JH. Copper binding to the octarepeats of the prion protein. Affinity, specificity, folding and cooperativity: insights from circular dichroism. J Biol Chem. 2003;278(9):6795–802.

Goldfarb LG, Brown P, McCombie WR, Goldgaber D, Swergold GD, Wills PR, et al. Transmissible familial Creutzfeldt-Jakob disease associated with five, seven, and eight extra octapeptide coding repeats in the PRNP gene. Proc Natl Acad Sci U S A. 1991;88(23):10926–30.

Guillot-Sestier MV, Sunyach C, Druon C, Scarzello S, Checler F. The alpha-secretase-derived N-terminal product of cellular prion, N1, displays neuroprotective function in vitro and in vivo. J Biol Chem. 2009;284(51):35973–86.

Harford C, Sarkar B. Amino terminal Cu(II)- and Ni(II)-binding (ATCUN) motif of proteins and peptides – metal binding, DNA cleavage, and other properties. Acc Chem Res. 1997;30(3):123–30.

Herms J, Tings T, Gall S, Madlung A, Giese A, Siebert H, et al. Evidence of presynaptic location and function of the prion protein. J Neurosci. 1999;19:8866–75.

Hornshaw MP, McDermott JR, Candy JM. Copper binding to the N-terminal tandem repeat regions of mammalian and avian prion protein. Biochem Biophys Res Comm. 1995a;207:621–9.

Hornshaw MP, McDermott JR, Candy JM, Lakey JH. Copper binding to the N-terminal tandem repeat region of mammalian and avian prion protein: structural studies using synthetic peptides. Biochem Biophys Res Commun. 1995b;214(3):993–9.

Jones CE, Klewpatinond M, Abdelraheim SR, Brown DR, Viles JH. Probing $copper^{2+}$ binding to the prion protein using diamagnetic $nickel^{2+}$ and 1H NMR: the unstructured N terminus facilitates the coordination of six $copper^{2+}$ ions at physiological concentrations. J Mol Biol. 2005;346(5):1393–407.

Kanaani J, Prusiner SB, Diacovo J, Baekkeskov S, Legname G. Recombinant prion protein induces rapid polarization and development of synapses in embryonic rat hippocampal neurons in vitro. J Neurochem. 2005;95(5):1373–86.

Klamt F, Dal-Pizzol F, Conte DA Frota ML Jr, Walz R, Andrades ME, Gomes DA Silva E, et al. Imbalance of antioxidant defense in mice lacking cellular prion protein. Free Radic Biol Med. 2001;30:1137–44.

Kong Q, Surewicz WK, Petersen RB, Zou W, Chen SG, Gambetti P, et al. Inherited prion diseases. In: Prusiner SB, editor. Prion biology and diseases. Cold Spring Harbor: Cold Spring Harbor Library Press; 2004. p. 673–775.

Kramer ML, Kratzin HD, Schmidt B, Romer A, Windl O, Liemann S, et al. Prion protein binds copper within the physiological concentration range. J Biol Chem. 2001;276:16711–9.

Kuffer A, Lakkaraju AK, Mogha A, Petersen SC, Airich K, Doucerain C, et al. The prion protein is an agonistic ligand of the G protein-coupled receptor Adgrg6. Nature. 2016;536(7617):464–8.

Leliveld SR, Dame RT, Wuite GJ, Stitz L, Korth C. The expanded octarepeat domain selectively binds prions and disrupts homomeric prion protein interactions. J Biol Chem. 2006;281(6):3268–75.

Leliveld SR, Stitz L, Korth C. Expansion of the octarepeat domain alters the misfolding pathway but not the folding pathway of the prion protein. Biochemistry. 2008;47(23):6267–78.

Liang J, Wang W, Sorensen D, Medina S, Ilchenko S, Kiselar J, et al. Cellular prion protein regulates its own alpha-cleavage through ADAM8 in skeletal muscle. J Biol Chem. 2012;287(20):16510–20.

Liu L, Jiang D, McDonald A, Hao Y, Millhauser GL, Zhou F. Copper redox cycling in the prion protein depends critically on binding mode. J Am Chem Soc. 2011;133(31):12229–37.

Markham KA, Roseman GP, Linsley RB, Lee HW, Millhauser GL. Molecular features of the Zn(2+) binding site in the prion protein probed by (113)Cd NMR. Biophys J. 2019;116(4):610–20.

McDonald AJ, Dibble JP, Evans EG, Millhauser GL. A new paradigm for enzymatic control of alpha-cleavage and beta-cleavage of the prion protein. J Biol Chem. 2013.

McDonald AJ, Leon DR, Markham KA, Wu B, Heckendorf CF, Schilling K, et al. Altered domain structure of the prion protein caused by Cu(2+) binding and functionally relevant mutations: analysis by cross-linking, MS/MS, and NMR. Structure. 2019;27(6):907–22. e905

McLennan NF, Brennan PM, McNeill A, Davies I, Fotheringham A, Rennison KA, et al. Prion protein accumulation and neuroprotection in hypoxic brain damage. Am J Pathol. 2004;165(1):227–35.

McMahon HE, Mange A, Nishida N, Creminon C, Casanova D, Lehmann S. Cleavage of the amino terminus of the prion protein by reactive oxygen species. J Biol Chem. 2001;276(3):2286–91.

Millhauser GL. Copper binding in the prion protein. Acc Chem Res. 2004;37(2):79–85.

Millhauser GL. Copper and the prion protein: methods, structures, function, and disease. Annu Rev Phys Chem. 2007;58:299–320.

Miura T, Sasaki S, Toyama A, Takeuchi H. Copper reduction by the octapeptide repeat region of prion protein: pH dependence and implications in cellular copper uptake. Biochemistry. 2005;44(24):8712–20.

Mouillet-Richard S, Ermonval M, Chebassier C, Laplanche JL, Lehmann S, Launay JM, et al. Signal transduction through prion protein. Science. 2000;289(5486):1925–8.

Nguyen XTA, Tran TH, Cojoc D, Legname G. Copper binding regulates cellular prion protein function. Mol Neurobiol. 2019;56(9):6121–33.

Pauly PC, Harris DA. Copper stimulates endocytosis of the prion protein. J Biol Chem. 1998;273:33107–19.

Perera WS, Hooper NM. Ablation of the metal ion-induced endocytosis of the prion protein by disease-associated mutation of the octarepeat region. Curr Biol. 2001;11(7):519–23.

Prusiner SB. Prion biology and diseases. Cold Spring Harbor Laboratory Press: Cold Spring Harbor; 2004.

Pushie MJ, Pickering IJ, Martin GR, Tsutsui S, Jirik FR, George GN. Prion protein expression level alters regional copper, iron and zinc content in the mouse brain. Metallomics Integr Biometal Sci. 2011;3(2):206–14.

Rachidi W, Vilette D, Guiraud P, Arlotto M, Riondel J, Laude H, et al. Expression of prion protein increases cellular copper binding and antioxidant enzyme activities but not copper delivery. J Biol Chem. 2003;278(11):9064–72.

Salzano G, Giachin G, Legname G. Structural consequences of copper binding to the prion protein. Cells. 2019;8(8)

Schilling KM, Tao L, Wu B, Kiblen JTM, Ubilla-Rodriguez NC, Pushie MJ, et al. Both N-terminal and C-terminal histidine residues of the prion protein are essential for copper coordination and neuroprotective self-regulation. J Mol Biol. 2020.

Shmerling D, Hegyi I, Fischer M, Blattler T, Brandner S, Gotz J, et al. Expression of amino-terminally truncated PrP in the mouse leading to ataxia and specific cerebellar lesions. Cell. 1998;93(2):203–14.

Solomon IH, Huettner JE, Harris DA. Neurotoxic mutants of the prion protein induce spontaneous ionic currents in cultured cells. J Biol Chem. 2010;285(34):26719–26.

Sonati T, Reimann RR, Falsig J, Baral PK, O'Connor T, Hornemann S, et al. The toxicity of anti-prion antibodies is mediated by the flexible tail of the prion protein. Nature. 2013.

Spevacek AR, Evans EG, Miller JL, Meyer HC, Pelton JG, Millhauser GL. Zinc drives a tertiary fold in the prion protein with familial disease mutation sites at the interface. Structure. 2013;21(2):236–46.

Stevens DJ, Walter ED, Rodriguez A, Draper D, Davies P, Brown DR, et al. Early onset prion disease from octarepeat expansion correlates with copper binding properties. PLoS Pathog. 2009;5(4):e1000390.

Stöckel J, Safar J, Wallace AC, Cohen FE, Prusiner SB. Prion protein selectively binds copper(II) ions. Biochemistry. 1998;37:7185–93.

Stys PK, You H, Zamponi GW. Copper-dependent regulation of NMDA receptors by cellular prion protein: implications for neurodegenerative disorders. J Physiol. 2012;590(Pt 6):1357–68.

Sunyach C, Cisse MA, da Costa CA, Vincent B, Checler F. The C-terminal products of cellular prion protein processing, C1 and C2, exert distinct influence on p53-dependent staurosporine-induced caspase-3 activation. J Biol Chem. 2007;282(3):1956–63.

Tobler I, Gaus SE, Deboer T, Achermann P, Fischer M, Rulicke T, et al. Altered circadian activity rhythms and sleep in mice devoid of prion protein. Nature. 1996;380(6575):639–42.

Valensin D, Luczkowski M, Mancini FM, Legowska A, Gaggelli E, Valensin G, et al. The dimeric and tetrameric octarepeat fragments of prion protein behave differently to its monomeric unit. Dalton Trans. 2004;9:1284–93.

Van Doorslaer S, Cereghetti GM, Glockshuber R, Schweiger A. Unraveling the Cu^{2+} binding sites in the C-terminal domain of the murine prion protein: a pulse EPR and ENDOR study. J Phys Chem. 2001;105:1631–9.

Veal EA, Day AM, Morgan BA. Hydrogen peroxide sensing and signaling. Mol cell. 2007;26(1):1–14.

Viles JH, Cohen FE, Prusiner SB, Goodin DB, Wright PE, Dyson HJ. Copper binding to the prion protein: structural implications of four identical cooperative binding sites. Proc Natl Acad Sci U S A. 1999;96:2042–7.

Waggoner DJ, Drisaldi B, Bartnikas TB, Casareno RLB, Prohaska JR, Gitlin JD, et al. Brain copper content and cuproenzyme activity do not vary with prion protein expression level. J Biol Chem. 2000;275:7455–8.

Walter ED, Chattopadhyay M, Millhauser GL. The affinity of copper binding to the prion protein octarepeat domain: evidence for negative cooperativity. Biochemistry. 2006;45(43):13083–92.

Walter ED, Stevens DJ, Visconte MP, Millhauser GL. The prion protein is a combined zinc and copper binding protein: Zn2+ alters the distribution of Cu2+ coordination modes. J Am Chem Soc. 2007;129(50):15440–1.

Walter ED, Stevens DJ, Spevacek AR, Visconte MP, Dei Rossi A, Millhauser GL. Copper binding extrinsic to the octarepeat region in the prion protein. Curr Protein Pept Sci. 2009.

Watt NT, Hooper NM. Reactive oxygen species (ROS)-mediated beta-cleavage of the prion protein in the mechanism of the cellular response to oxidative stress. Biochem Soc Trans. 2005;33(Pt 5):1123–5.

Watt NT, Taylor DR, Kerrigan TL, Griffiths HH, Rushworth JV, Whitehouse IJ, et al. Prion protein facilitates uptake of zinc into neuronal cells. Nat Commun. 2012;3:1134.

Watt NT, Griffiths HH, Hooper NM. Neuronal zinc regulation and the prion protein. Prion. 2013;7(3):203–8.

Wu B, McDonald AJ, Markham K, Rich CB, McHugh KP, Tatzelt J, et al. The N-terminus of the prion protein is a toxic effector regulated by the C-terminus. Elife. 2017;6

Yadavalli R, Guttmann RP, Seward T, Centers AP, Williamson RA, Telling GC. Calpain-dependent endoproteolytic cleavage of PrPSc modulates scrapie prion propagation. J Biol Chem. 2004;279(21):21948–56.

You H, Tsutsui S, Hameed S, Kannanayakal TJ, Chen L, Xia P, et al. Abeta neurotoxicity depends on interactions between copper ions, prion protein, and N-methyl-D-aspartate receptors. Proc Natl Acad Sci U S A. 2012;109(5):1737–42.